PCP
PLANT & CELL PHYSIOLOGY

Localization and Quantification of Callose in the Streptophyte Green Algae *Zygnema* and *Klebsormidium*: Correlation with Desiccation Tolerance

Klaus Herburger[1] and Andreas Holzinger*[1]

[1]University of Innsbruck, Institute of Botany, Functional Plant Biology, Sternwartestrasse 15, 6020 Innsbruck, Austria
*Corresponding author: Andreas Holzinger, E-mail, Andreas.Holzinger@uibk.ac.at; Fax, +0043-512-507-51099.
(Received July 21, 2015; Accepted September 18, 2015)

Regular Paper

Freshwater green algae started to colonize terrestrial habitats about 460 million years ago, giving rise to the evolution of land plants. Today, several streptophyte green algae occur in aero-terrestrial habitats with unpredictable fluctuations in water availability, serving as ideal models for investigating desiccation tolerance. We tested the hypothesis that callose, a β-D-1,3-glucan, is incorporated specifically in strained areas of the cell wall due to cellular water loss, implicating a contribution to desiccation tolerance. In the early diverging genus *Klebsormidium*, callose was drastically increased already after 30 min of desiccation stress. Localization studies demonstrated an increase in callose in the undulating cross cell walls during cellular water loss, allowing a regulated shrinkage and expansion after rehydration. This correlates with a high desiccation tolerance demonstrated by a full recovery of the photosynthetic yield visualized at the subcellular level by Imaging-PAM. Furthermore, abundant callose in terminal cell walls might facilitate cell detachment to release dispersal units. In contrast, in the late diverging *Zygnema*, the callose content did not change upon desiccation for up to 3.5 h and was primarily localized in the corners between individual cells and at terminal cells. While these callose deposits still imply reduction of mechanical damage, the photosynthetic yield did not recover fully in the investigated young cultures of *Zygnema* upon rehydration. The abundance and specific localization of callose correlates with the higher desiccation tolerance in *Klebsormidium* when compared with *Zygnema*.

Keywords: Aero-terrestrial green algae • Cell wall • Evolutionary biology • Imaging-PAM • Phylogeny • Terrestrialization.

Abbreviations: AB, antibody; AGP, arabinogalactan protein; AH, ambient humidity; BSA, bovine serum albumin; CLSM, confocal laser scanning microscopy; NIR, near infrared; PBS, phosphate-buffered saline; Y(II), effective quantum yield of PSII.

Introduction

In contrast to land plants, thalli of streptophyte green algae are not protected by watertight covering tissues such as cutinized epidermal layers, periderm or bark (Graham et al. 2009). Nevertheless, some of these green algae occur in aero-terrestrial habitats, where they are frequently exposed to desiccating conditions causing drastic mechanical deformations of the cell wall and protoplast (Holzinger and Karsten 2013). As many of these green algae occur worldwide (Lewis and McCourt 2004, Leliaert et al. 2012), numerous studies investigated the physiological adaptions of aero-terrestrial streptophyte green algae to their habitats (Hawes 1990, Elster and Benson 2004, Gray et al. 2007, Karsten and Rindi 2010, Karsten et al. 2010, Holzinger et al. 2011, Kaplan et al. 2012, Aigner et al. 2013, Karsten et al. 2013, Kaplan et al. 2013, Karsten and Holzinger 2014, Pichrtová et al. 2014a, Pichrtová et al. 2014b, Vilumbrales et al. 2014, Herburger et al. 2015). Despite detailed knowledge on the composition of the cell walls of streptohyte algae being available (Domozych et al. 2012), the contribution of these walls to coping with harsh environmental conditions is very limited so far. This is surprising, as the extracellular matrix is the only barrier between the algal protoplasts and the environment.

In the past decade, research has focused on the architecture and chemical composition of cell walls in unicellular Zygnematophyceae, a late diverged streptophyte green algae lineage which founded the line of embryophytes after colonizing terrestrial habitats about 460 million years ago (Wickett et al. 2014), by using immunocytochemistry and focusing on pectins (Domozych et al. 2007, Eder and Lütz-Meindl 2008, Domozych et al. 2009, Eder and Lütz-Meindl 2010, Domozych et al. 2011, Domozych et al.2014) or hemicelluloses (Eder et al. 2008, Domozych et al. 2009), or by the use of general polysaccharide staining (Brosch-Salomon et al. 1998). High-throughput techniques such as glycan microarrays gave semi-quantitative insights into the occurrence of cell wall components in several green algae (Sørensen et al. 2011). These findings were set into an evolutionary context to show significant differences between early- (e.g. Klebsormidiophyceae) and late-branching (e.g. Zygnematophyceae) streptophyte green algae and land plants (Popper and Tuohy 2010, Domozych et al. 2012). Recently, transcriptome and genome analysis of species belonging to the Klebsormidiophyceae (Wodniok et al. 2011, Timme et al. 2012, Holzinger et al. 2014, Hori et al. 2014) and Zygnematophyceae (Timme et al. 2012) also became available. These data sets were mined for enzymes involved in cell wall biosynthesis and compared with land plants, confirming their

Plant Cell Physiol. 56(11): 2259–2270 (2015) doi:10.1093/pcp/pcv139, Advance Access publication on 26 September 2015, available online at www.pcp.oxfordjournals.org

most important core cell wall polysaccharides to be already present in some streptophyte green algae (Mikkelsen et al. 2014, Yin et al. 2014).

Similar to land plants, the cell walls of Zygnematophyceae comprise load-bearing compounds such as cellulose and hemicelluloses (Scheller and Ulvskov 2010, Sørensen et al. 2011), matrix carboxylic polysaccharides (i.e. pectins; Popper et al. 2011) and glycoproteins [arabinogalactan proteins (AGPs), extensins and expansins (Vannerum et al. 2011, Domozych et al. 2012]. In contrast, most of the cell wall polymers usually found in the Zygnematophyceae and land plants are absent in the Klebsormidiophyceae (Sørensen et al. 2011). However, both classes contain callose, a β-D-1,3-glucan (Bacic et al. 2009). Biosynthesis of callose is catalyzed by family 48 glycosyltransferases (Cantarel et al. 2009), which is part of a very ancient eukaryotic pathway (Michel et al. 2010). It occurs in many land plants as a regular component of developing cell plates during cytokinesis (Verma 2001), in pollen walls and tubes (Dong et al. 2005, Nishikawa et al. 2005, Shi et al. 2014) and in sieve elements (Chen and Kim 2009), and it acts as a regulator of plasmodesmata for controlling the movement of molecules through the symplasmic continuum (Chen and Kim 2009). Callose is involved in many stress responses, such as plugging plasmodesmata or to prevent pathogen spread throughout the plant (Iglesias et al. 2000, Eggert et al. 2014). It is incorporated within minutes after cellular damage due to mechanical strain, heavy metal treatment or stress caused by plasmolysis and temperature fluctuations (Bhuja et al. 2004, Bacic et al. 2009). In several green algae, callose was found in newly formed septae during cytokinesis (Scherp et al. 2001), the chamber walls of developing meiospores in *Coleochaete* (Graham and Taylor 1986), in rhizoids and conjugation tubes of *Spirogyra* (Yamada et al. 2003), and it is incorporated after ultrasonic treatment (Scherp et al. 2001). However, knowledge of the contribution of callose to the aero-terrestrial lifestyle of green algae is lacking.

In the present study, we employed immunocytochemistry in live cells as well as in high-pressure frozen cells. Additionally, standard staining procedures and spectrofluorimetry were used to visualize and quantify the change of callose content after experimental desiccation stress. The physiological status of the desiccated and recovered individual algal filaments was monitored by Imaging-PAM measurements. As desiccation stress causes drastic cell wall deformations and callose is involved in many wound responses related to mechanical strain, we hypothesize that it is incorporated in deformed areas of the cell wall. This would imply an important contribution to desiccation tolerance. Flexible cell walls are crucial for surviving cellular water loss by allowing regulated shrinkage of the protoplast (Holzinger et al. 2011), as shown for desiccation-tolerant 'resurrection plants', lichens, seeds and the intertidal macroalgae *Ulva* (Webb and Arnott 1982, Brown et al. 1987, Moore et al. 2013, Holzinger et al. 2015). We have chosen two species of filamentous green algae from the class Klebsormidiophyceae [*Klebsormidium crenulatum* (Karsten et al. 2010, Kaplan et al. 2012) and *Klebsormidium nitens* (Kaplan et al. 2012)] and two species from the class Zygnematophyceae [*Zygnema* sp. 'Saalach' (S) and *Zygnema* sp. 'Elmau-Alm' (E-A) (Herburger et al. 2015)]. As each of these species is assigned to different subclades within the respective genus (Kaplan et al. 2012, Herburger et al. 2015), both genera investigated are represented on a broad phylogenetic base. This enabled us to put the findings on the role of callose for an aero-terrestrial lifestyle in an evolutionary context, by comparing early-branching Klebsormidiophyceae with the later branching Zygnematophyceae.

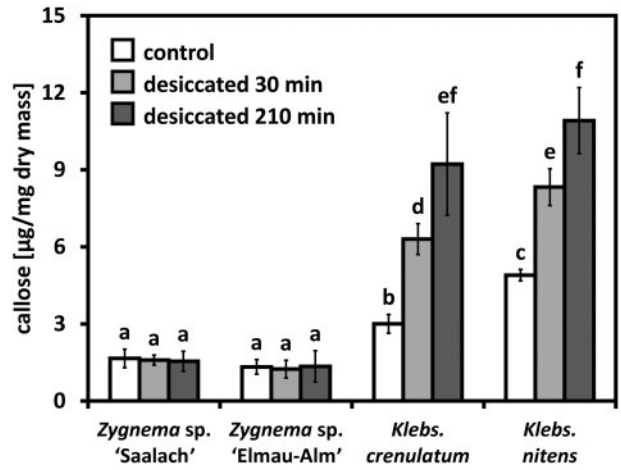

Fig. 1 Comparison of the callose content in two *Zygnema* and *Klebsormidium* strains (control and desiccated for 30 and 210 min) determined by colorimetric quantification ($n = 4 \pm$ SD). Callose content is expressed in µg of pachyman equivalents per mg of algal dry mass. Significant differences between groups are indicated by lower case letters. Data were analyzed by one-way ANOVA followed by Tukey's post-hoc test ($P < 0.001$).

Results

Spectrofluorimetric quantification of callose

Control samples of *Zygnema* contained between half and a third of the amount of callose when compared with *Klebsormidium* (**Fig. 1**). Desiccation for up to 210 min did not change the callose content in *Zygnema* (**Fig. 1**; **Supplementary Table S1**). In contrast, 30 min of desiccation increased the callose content in *K. crenulatum* and *K. nitens* significantly by 109.8 ± 9.5% and 70.0 ± 8.6%, respectively (**Fig. 1**). Desiccation for 210 min led to an even stronger increase compared with the initial value: 207.2 ± 21.6% and 122.9 ± 11.8% in *K. crenulatum* and *K. nitens*, respectively (**Fig. 1**).

Desiccation effects, Calcofluor white and Aniline blue staining

To visualize the effect of cellular water loss on algal cell morphology already after 30 min of desiccation, we used confocal laser scanning microscopy (CLSM) and Chl autofluorescence (**Fig. 2**). In both *Zygnema* (**Fig. 2A-D**) and *Klebsormidium* (**Fig. 2E–J**), desiccation resulted in a drastic deformation of the cell walls and protoplasts (**Fig. 2**). In *Zygnema*, the longitudinal cell walls

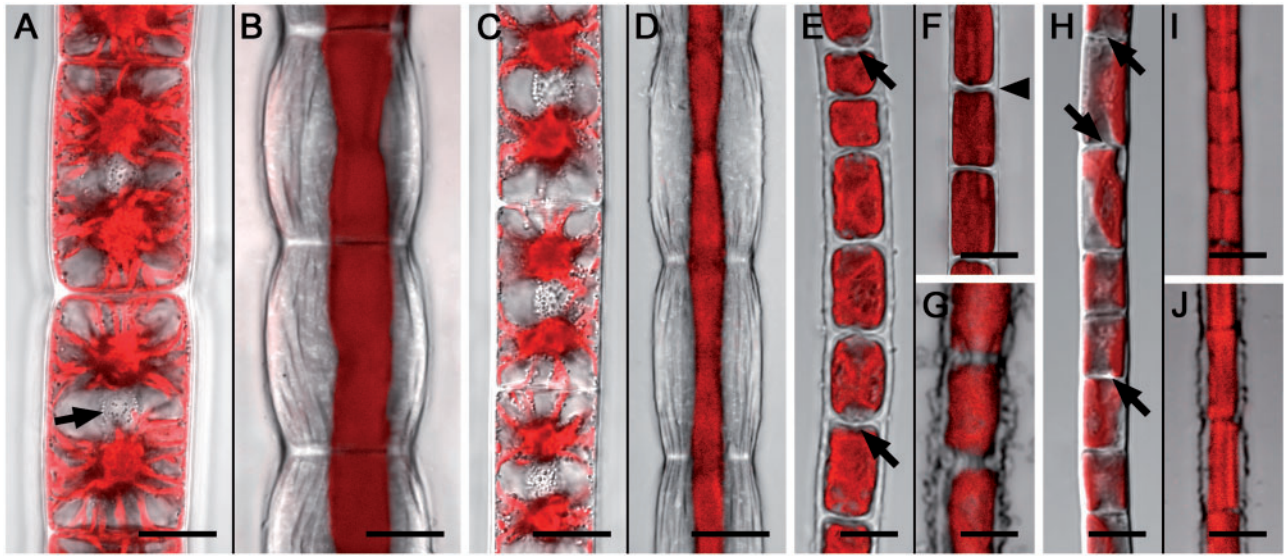

Fig. 2 Confocal laser scanning micrographs of *Zygnema* S (A, B), *Zygnema* E-A (C, D), *Klebsormidium crenulatum* (E–G) and *Klebsormidium nitens* (H–J). Controls (A, C, E, H) and desiccated (30 min at ambient humidity; B, D, F, G, I, J) algal cell filaments. Chl autofluorescence is shown in red. (A) Protoplasts closely attached to the cell wall, two stellate chloroplasts and a centrally located nucleus per cell (arrow). (B) Longitudinal cell walls convexly expanded with conspicuous undulations, cross cell walls not deformed; protoplasts retracted from the longitudinal cell walls. (C) Hydrated cells with two stellate chloroplasts and central nuclei. (D) Retracted protoplasts and deformed longitudinal cell walls. (E) Hydrated cells with parietal single chloroplasts, protuberances in cross walls (arrows). (F) Desiccated filament with reduced diameter, undulated cross cell walls (arrowhead), protoplasts closely attached to the cell wall (arrows). (G) The longitudinal cell walls appear frayed. (H) Protuberances of wall material in the cross cell walls are indicated by arrows. (I) Desiccated filament with reduced diameter. (J) Frayed longitudinal cell walls. Scale bar = 10 μm (A–D); 5 μm (E–J).

expanded convexly, showed conspicuous convolutions along the longitudinal axis, but did not rupture (**Fig. 2B, D**). In contrast, the cross cell walls retained their shape and the diameter of the cell filaments was not drastically reduced (**Fig. 2B, D**). Cellular water loss caused retraction of the initially turgescent protoplasts from the outer cell walls (**Fig. 2B, D**), while they stayed partially attached to the cross walls, mostly in the cell center (**Fig. 2B, D**). In *Klebsormidium*, desiccation led to shrinkage, indicated by cell filaments reducing their initial diameter and cross cell walls becoming undulated, while the longitudinal walls were not deformed (**Fig. 2F, I**). Occasionally (<20%), filaments of both *Klebsormidium* strains did not reduce their diameter upon desiccation and their longitudinal cell walls appeared frayed (**Fig. 2G, J**). Some cross cell walls in *Klebsormidium* exhibited centrally located protuberances (**Fig. 2E, H**). Staining with Aniline blue (**Fig. 3**) and Calcofluor white (**Supplementary Fig. S1**) revealed callose and cellulose in the cell walls of *Zygnema* and *Klebsormidium*. In *Zygnema*, callose was restricted to the cell corners between individual cells and convexly expanded terminal walls (**Fig. 3**). In contrast, most cross cell walls in *Klebsormidium* showed strong fluorescence, with a maximum in the central protuberances, when developed (**Fig. 3**). In *Zygnema* S, after Calcofluor white staining the longitudinal and cross cell walls of older (i.e. longer) cells showed strong fluorescence, while staining was weak between younger recently divided (i.e. shorter) cells (**Supplementary Fig. S1A**). The Calcofluor fluorescence signal appeared weaker in the cross walls of *Zygnema* E-A (**Supplementary Fig. S1B**). Again, the longitudinal cell walls exhibited fluorescence and the strongest signal was detected in the cell corners (**Supplementary Fig. S1B**). *Klebsormidium* in general showed weaker fluorescence compared with *Zygnema* (**Supplementary Fig. S1C, D**). However, Calcofluor white fluorescence was detected in longitudinal and most cross cell walls of *K. crenulatum* (**Supplementary Fig. S1C**) and in the cross walls of *K. nitens*, where the strongest signal occurred in central protuberances (**Supplementary Fig. S1D**).

Immunocytochemistry

Live cell labeling with the monoclonal antibody (AB) 400-2 allowed a specific detection of callose in *Zygnema* (**Fig. 4**) and *Klebsormidium* (**Fig. 5**). Hydrated filaments of both *Zygnema* S and *Zygnema* E-A showed a similar pattern of callose distribution: callose was abundant in terminal cross cell walls (**Fig. 4A, B**) and in detaching or deformed parts of the walls (**Fig. 4C, D**). Despite long incubation times, AB penetration into unexposed cross cell walls was not satisfactory. Therefore, we labeled semi-thin sections of high-pressure-fixed algae (**Fig. 4E–H**). There, the callose signal usually was restricted to cell corners between the cells of control *Zygnema* filaments (**Fig. 4E, F**). In shorter, i.e. younger, cells, the cross cell walls also contained callose (**Fig. 4E, F**). Similarly, desiccated *Zygnema* filaments exhibited callose-rich cell corners and terminal cross cells, while the unexposed cross and longitudinal cell walls lacked callose (**Fig. 4G, F**). Occasionally, desiccated cells of *Zygnema* E-A with protoplasts closely attached to the wall contained abundant callose in the longitudinal cell walls (**Supplementary Fig. S2**). In *K. crenulatum*, live cell labeling

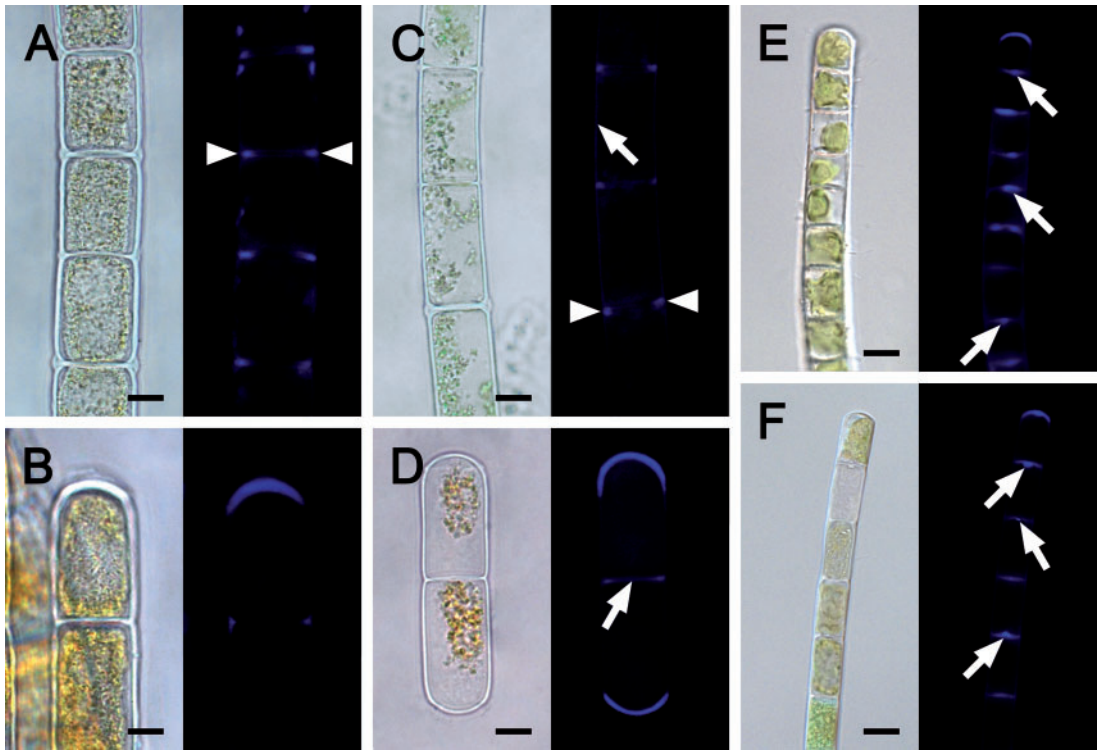

Fig. 3 Light and corresponding Aniline blue-stained fluorescence (callose) micrographs of *Zygnema* S (A, B), *Zygnema* E-A (C, D), *Klebsormidium crenulatum* (E) and *Klebsormidium nitens* (F). (A) Callose in the cell corners between individual cells (arrowheads). (B) Abundant callose accumulation in the terminal cell wall. (C) Callose in the corners between individual cells (arrowheads); lateral wall with less signal (arrow). (D) Fragmented filament with callose accumulation in convex terminal walls; cross wall with less signal (arrow). (E) Abundant callose in cross walls, with a maximum in the center (arrows) and in the terminal wall. (F) Callose in the terminal cell wall and in protuberances of cross cell walls (arrows). Scale bar = 10 μm (A–D); 5 μm (E, F).

showed callose to be abundant in cell corners and terminal cell walls (**Fig. 5A**), while in *K. nitens* it was mainly restricted to terminal walls (**Fig. 5B**), and after cell detachment in newly exposed cross cell walls (**Fig. 5C**) and deformed cells (**Fig. 5D**). Labeling of semi-thin sections of hydrated *Klebsormidium* filaments revealed callose occurring in cell corners and in most unexposed cross cell walls (**Fig. 5E, F**), while after desiccation the cell corners and undulated cross cell walls were rich in callose (**Fig. 5G, H**). Moreover, desiccated filaments of *K. nitens* showed a dotted callose distribution in the longitudinal cell walls (**Fig. 5H**). Negative control samples after omitting incubation with the primary AB showed no staining due to a lack of binding of the secondary AB (**Supplementary Fig. S3A–E**).

Immunogold labeling

Labeling of callose epitopes with 10 nm gold particles on ultrathin sections showed callose throughout the cross cell walls of *K. crenulatum* and also in the centrally located protuberances (**Fig. 6A**) and particularly in the terminal cell walls of *K. nitens* (**Fig. 6B**).

Imaging-PAM

To exclude that the drastic deformation of the cells and protoplasts after desiccation is lethal, we used the microscopic version of an Imaging-PAM to monitor the effective quantum yield of PSII [Y(II)] prior to and after desiccation and upon rehydration (**Figs. 7**, **8**). In *Zygnema* S and *Zygnema* E-A, 30 min of desiccation caused a strong reduction of the Y(II) in all cells from approximately 0.65 to approximately 0.25 and from approximately 0.60 to 0.15, respectively (**Fig 7A, B**). Subsequent rehydration allowed the cells of both *Zygnema* strains to restore their initial shape and the Y(II) to recover homogenously to about half of the initial value (**Fig. 7A**, B), while *Zygnema* S cells with thicker cross cell walls showed the highest Y(II) after 180 min of recovery (**Fig. 7A**). Furthermore, after 180 min, the characteristic stellate shape of the two chloroplasts was remodeled in several cells (**Fig. 7A, B**). The cells of *K. crenulatum* within one filament exhibited a similar Y(II), which declined after desiccation from approximately 0.65 to approximately 0.35 (**Fig. 8A**). In contrast, the Y(II) in *K. nitens* varied between the cells of one filament (∼0.45 to ∼0.60; **Fig. 8B**). Thirty minutes of desiccation reduced the Y(II) uniformly to approximately 0.35 (**Fig. 8B**). Rehydration allowed both *Klebsormidium* strains to recover their Y(II) almost fully, and the filaments expanded to the initial value (**Fig. 8A, B**). In both *Klebsormidium* strains, the shape of the parietal chloroplast was restord after rehydration for 10 min (**Fig. 7A, B**). The Y(II) in terminal cells of fragmented *Zygnema* and *Klebsormidium* filaments and small fragments (2–3 cells) of

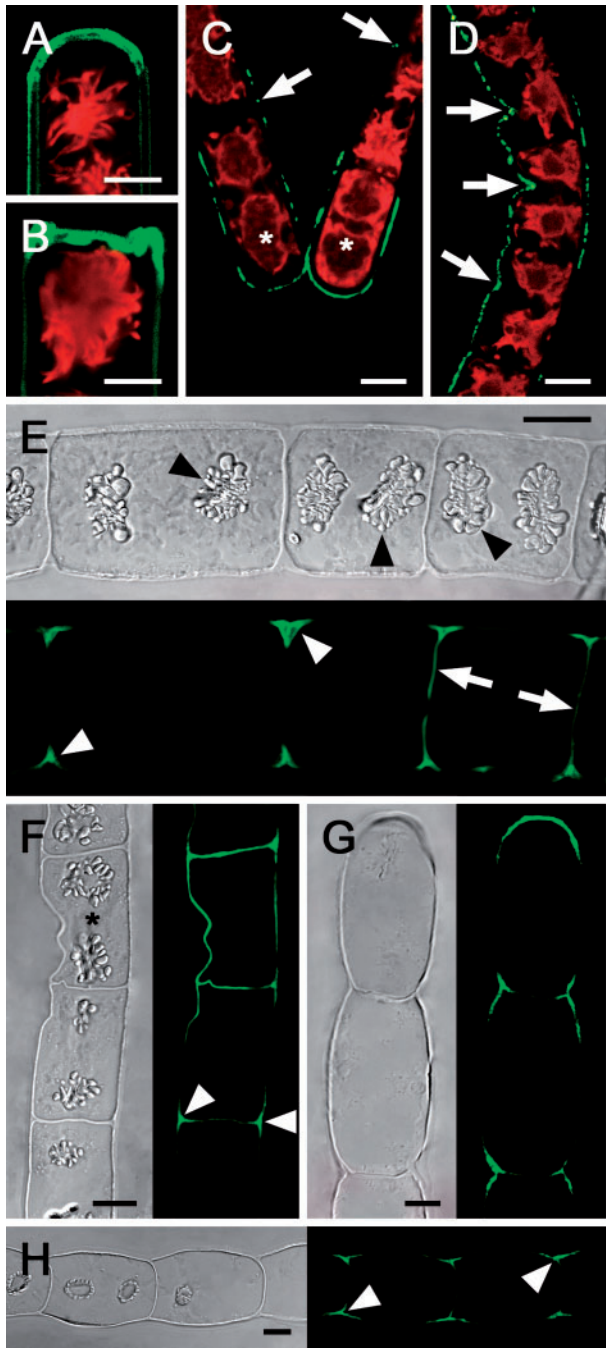

Fig. 4 Micrographs of *Zygnema* S (A, B, E, G) and *Zygnema* E-A (C, D, F, H); hydrated cells (A–F), 210 min desiccated cells (G, H). (A–D) Live cell labeling (red, Chl autofluorescence); (E–H) the corresponding bright field image and labeling of semi-thin sections with the monoclonal antibody 400-2 (green). (A) Convex terminal cross wall stained abundantly. (B) Recently fragmented cells with massive staining in the new terminal wall. (C) Detaching filament; a strong signal in the terminal cells (asterisks) and weak labeling in longitudinal walls (arrow). (D) Filament with a deformed longitudinal cell wall abundantly stained (arrow). (E) Filament with clearly visible starch grains in pyrenoids (arrowheads); cell corners show strong labeling; only cross cell walls of young cells are stained (arrow). (F) Filament with a deformed cell (asterisk) and strong callose labeling in the area of deformation and in cell corners (arrowheads). (G) Desiccated filament with labeling restricted to the terminal cell wall and cell corners. (H) Desiccated filament with labeling in cell corners. Scale bar = 10 μm.

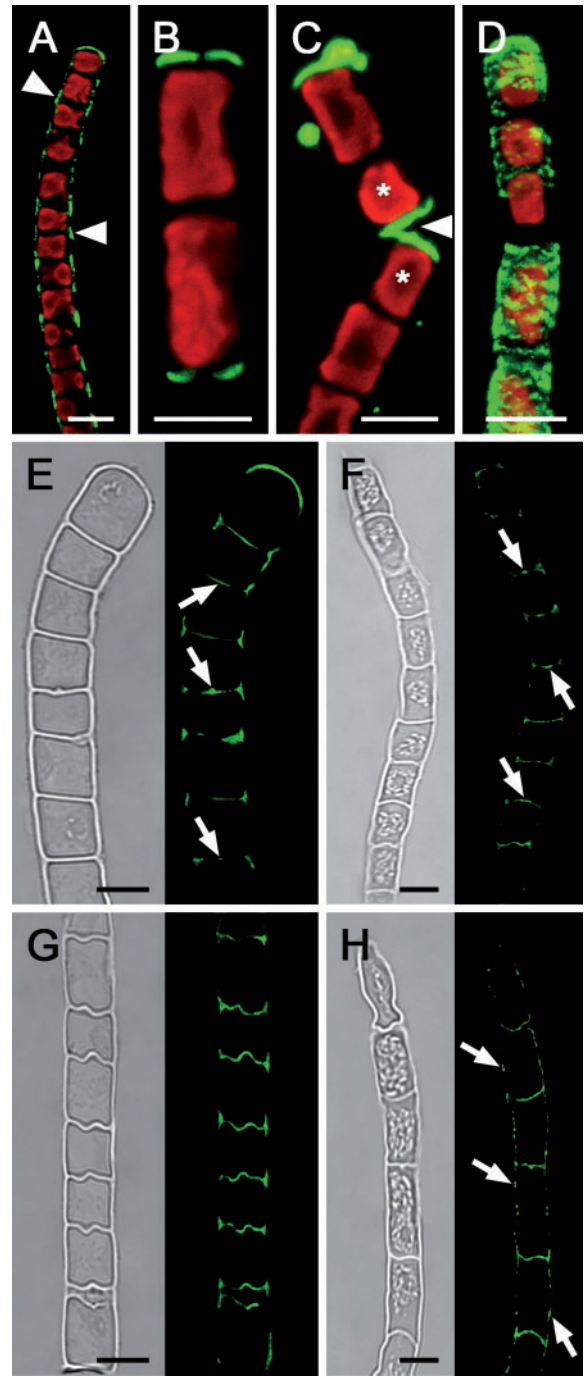

Fig. 5 Micrographs of *Klebsormidium crenulatum* (A, E, G) and *Klebsormidium nitens* (B, C, D, F, H). (A–D) Live cell labeling (red, Chl autofluorescence), and labeling of sem-ithin sections (E–H) of hydrated (E, F) and desiccated filaments (G, H) with the monoclonal AB 400-2 (green). Bright field image and corresponding labeling is shown. (A) Callose labeling in the longitudinal cell walls between individual cells (arrowheads). (B) Filament fragment with callose labeling in the terminal cross cell walls. (C) Detached cells (asterisks) show labeling in the terminal walls (arrowhead). (D) 3D projection of a deformed cell filament with strong callose labeling. (E) Callose labeling in cross cell walls, with maximal labeling in the center of the cross cell walls and protuberances (arrows). (F) Callose in the center of cross cell walls (arrows). (G) Undulated cross cell walls with abundant callose staining. (H) Callose labeling in cross cell walls and longitudinal walls (arrows). Scale bar = 5 μm.

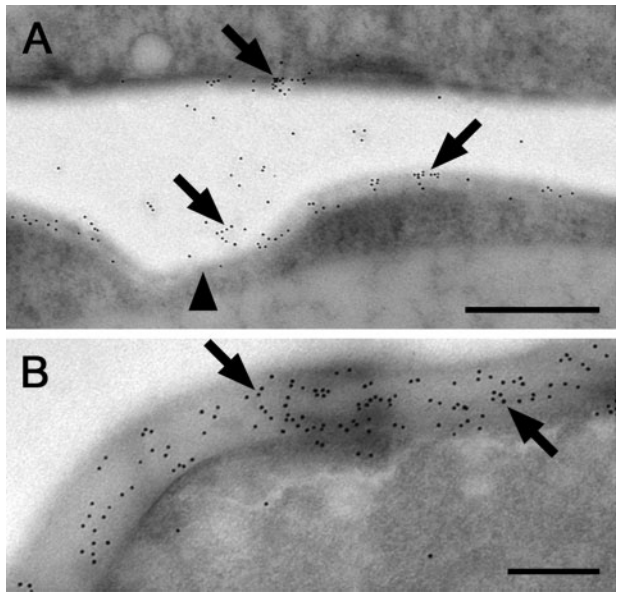

Fig. 6 Immunogold localization of callose epitopes (AB 400-2) in transmission electron micrographs of *Klebsormidium crenulatum* (A) and *Klebsormidium nitens* (B). (A) Cross cell wall and protuberance (arrowhead) stained by 10 nm gold particles (arrows). (B) Terminal cross cell with abundant binding of 10 nm gold particles (arrows) throughout the terminal cell wall. Scale bar = 500 nm (A); 200 nm (B).

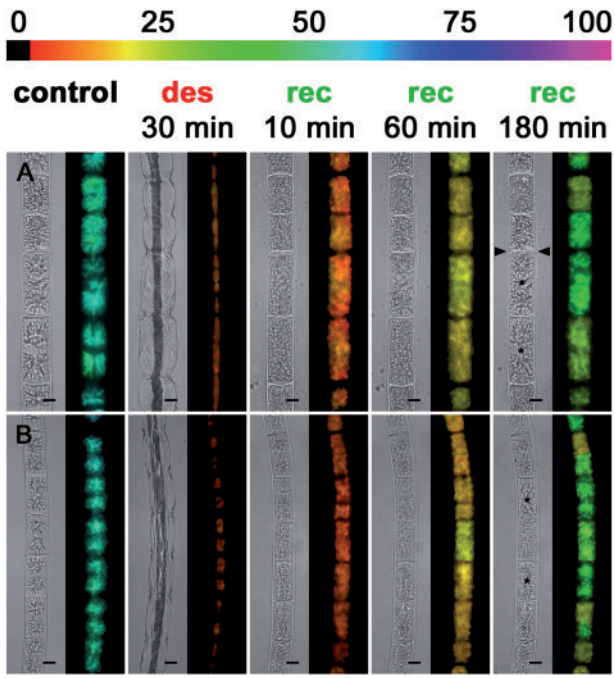

Fig. 7 Imaging-PAM micrographs of *Zygnema* S (A) and *Zygnema* E-A (B), near infrared (NIR) remission image and corresponding Y(II) images (false colored) (control, after 30 min of desiccation at ambient humidity and after 10, 60 and 180 min recovery). The color bar at the top indicates the relative Y(II) as a percentage. (A) After recovery for 180 min, cells with thicker cross cell walls (arrowheads) show the highest Y(II) and in some cells the characteristic stellate chloroplasts appear again (asterisks). (B) The stellate chloroplasts appear again after 180 min (asterisks). Scale bar = 10 μm.

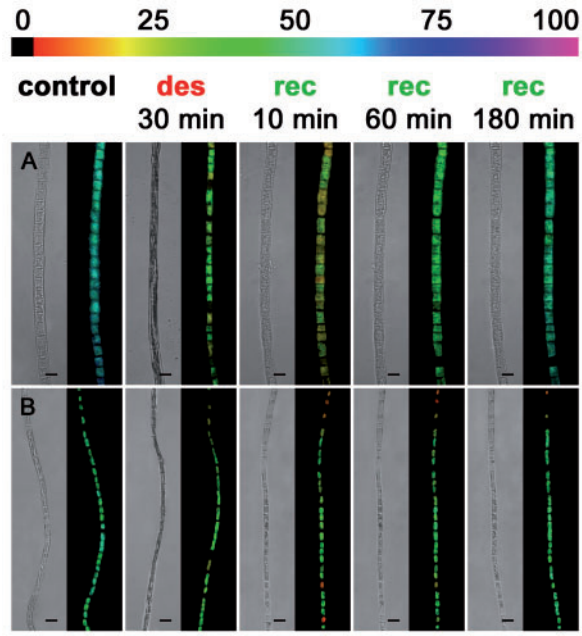

Fig. 8 Imaging-PAM micrographs of *Klebsormidium cernulatum* (A) and *Klebsormidium nitens* (B), near infrared (NIR) remission image and corresponding Y(II) images (false color) of algal filaments (control, after 30 min of desiccation at AH and after 10, 60 and 180 min of recovery). The color bar at the top indicates the relative Y(II) as a percentage. Scale bar = 10 μm.

K. nitens was similar to that of adjacent cells in long filaments (**Supplementary Fig. S4A–D**).

Discussion

Desiccation usually leads to a clearly visible deformation of plant cell walls (Moore et al. 2006, Holzinger et al. 2011). While the walls of some species exhibit a random wrinkling leading to irreversible damage, others show highly regular and reversible shrinking patterns (Brown et al. 1987, Moore et al. 2008), which is important for surviving cellular water loss (Webb and Arnott 1982). As information on deformable cell walls in algae is scarce, we used spectrofluormetry and immunocytochemistry to estimate the role of callose in coping with mechanical stress of the algal cell wall and protoplast during desiccation. Recently, in a transcriptomic analysis, callose synthase complex (UNO 39686, KEGG orthology: K 11000, EC 2.4.1.-) was found to be up-regulated by approximately 1.5-fold upon severe desiccation stress in *K. crenulatum* (Holzinger et al. 2014). This key enzyme has also been detected in the genome of *K. flaccidum* (gene family number OG00420; biological process category GO: 0052544—defence response by callose deposition in cell wall; Hori et al. 2014). It has to be emphasized that in our study, callose was not only detected as a stress response, but is already present in mechanically undisturbed algal filaments.

Callose allows a regulated shrinking process in *Klebsormidium*

We found a high abundance of callose in the cross walls of *Klebsormidium* filaments which allow a regulated reduction

of the cell filament diameter during cellular water loss. The longitudinal cell walls stayed closely attached to the protoplasts. This is crucial for preserving the structural integrity of the basic cell organelles (Holzinger et al. 2011), maintaining the turgor pressure and a high photosynthetic performance during short-term desiccation, as shown by microscopic Imaging-PAM. Furthermore, as the plasma membrane did not retract from the cell wall, additional callose can be incorporated during water loss to repair local injuries of the walls. This is indicated by higher callose contents and stronger AB labeling throughout the cross cell walls in both *Klebsormidium* species after desiccation. Furthermore, in *K. nitens*, callose was incorporated in the longitudinal cell walls after desiccation, pointing to local repairs of strained areas. In contrast to land plants, algae do not form wound-induced regenerative tissues, and therefore maintaining the integrity of individual cells is particularly important (Menzel 1988). In Desmidiaceae, wound plug formation after experimental microinjection has been shown to occur within 15 min (Holzinger et al. 1995), and even when cell development is supressed, e.g. by an G-actin-binding protein, the wound plug is formed undisturbed (Holzinger et al. 1997). Sometimes, cross cell walls in older or field-collected filaments of *K. crenulatum* become thick and multilayered due to the mode of cell division (Mikhailyuk et al. 2014). We demonstrate marked callose staining by Aniline blue as well as AB labeling in the corners between individual *Klebsormidium* cells. This finding is in agreement with observations of Mikhailyuk et al. (2014), who demonstrated triangular spaces of unidentified content in transmission electron microscopy samples. As shown moreover by immunogold labeling in 1-month-old cell filaments, callose occurs throughout the central part of cross cell walls and in the central protuberances of *K. crenulatum* and the terminal walls of *K. nitens*. The function of these protuberances remains largely unknown; they have also previously been shown in the Klebsormidiophyceae *Entransia* (Cook 2004). These structures could contribute to the fragmentation of the filaments, but are clearly distinct from the cylinders of cell wall material found during the division process in Desmidiaceae (Hall et al. 2008), which have been immunologically shown to contain highly methylesterified homogalacturonans in *Desmidium swartzii* (Andosch et al. 2015).

In natural habitats, green algae occurring in soil crusts strongly depend on rainwater as a source of available moisture. Rainwater is hypotonic compared with the cytoplasm of *Klebsormidium*, which exhibits a very negative osmotic potential (*K. crenulatum* = −2.09 MPa, *K. nitens* = −1.67 MPa; Kaplan et al. 2012) compared with obligatory submersed living green algae. These osmotic values are an adaptation to habitats with low water availability (Holzinger and Karsten 2013). A sharp osmotic gradient causes a rapid water uptake of desiccated protoplasts, while the closely attached cell walls act as an antagonist to the increasing turgor and prevent harmful expansion rates causing rupture of the plasma membrane. In desiccation-tolerant resurrection plants and the intertidal green macroalga *Ulva compressa*, maintaining flexible cell walls is also important for efficient rehydration (Moore et al. 2013, Holzinger et al. 2015). The processes in *U. compressa* are different, as inner pectic layers are responsible for the flexibility of the extremely thick cell walls; however, the effect, i.e. avoidance of mechanical damage, is similar. As shown by microscopic Imaging-PAM, rehydration of single algal filaments allowed photosynthesis to recover almost fully after 1 h (*K. nitens*) or 3 h (*K. crenulatum*), respectively. In part, this might be related to the morphology of the parietal chloroplast in *Klebsormidium*, which we consider as another adaption to changing filament diameters during desiccation and rehydration cycles: the chloroplast is shaped like an incompletely closed tube. Thus reducing the cell diameter during desiccation allows the margins of the chloroplast to become closely attached to each other (**Supplementary Fig. S5**). Near infrared (NIR) remission images of rehydrated *Klebsormidium* filaments revealed a similar chloroplast morphology to that prior to desiccation. This supports that the chloroplast ultrastructure in *K. crenulatum* remains intact even after desiccation for 4 d at 5% relative humidity (Holzinger et al. 2011).

Rapid incorporation of callose in response to deformation (e.g. perturbation) also occurs in Embryophytes (Bacic et al. 2009). In resurrection plants, arabinose-rich cell wall components in particular contribute to the cell wall's flexibility (Moore et al. 2013). However, as shown by glycan microarray analysis (Sørensen et al. 2011), cell walls of *Klebsormidium* lack these polymers. Furthermore, pectic substances related to cell wall flexibility in desmidiacean green algae [methylesterified homogalacturonan (HG); Eder and Lütz-Meindl 2008] and wall loosening in land plants (demethylesterfied homogalacturonans; Peaucelle et al. 2011) are absent in *Klebsormidium*. Klebsormidiophyceae lack most of the components (e.g. extensin) that are typical for cell walls of Embryophytes and late-branching streptophyte green algae (Domozych et al. 2012). However, the walls of *Klebsormidium* contain cellulose, which was visualized in the present study by Calcofluor white staining, where fluorescence was found in the cross cell walls while the longitudinal walls exhibit rather weak fluorescence. However, due to the non-specifity of calcofluor staining, callose-rich cell wall areas (e.g. centers of cross cell walls) are also likely to be be stained (Krishnamurthy 1999). The low amount of load-bearing cell wall components in *Klebsormidium* (i.e. cellulose and hemicelluloses), which was also reported previously (Domozych et al. 1980, Sørensen et al. 2011), probably reduces the cell wall's rigidity. Another cell wall-related factor supporting desiccation tolerance is mucilage layers (Shephard 1987). As discussed for *Interfilum* strains, these layers increase the water-holding capacity of the cells and contribute to a higher photosynthetic performance during desiccation stress (Karsten et al. 2014). Species of *Klebsormidium* belonging to clades E (*K. nitens*), B and G also form a mucilage envelope by gelatinization of the parental wall, while members of the clades D, F (*K. crenulatum*) are not coated by such layers (Rindi et al. 2011, Mikhailyuk et al. 2014). As on the filament level both *K. crenulatum* and *K. nitens* show similar responses to desiccation stress followed by rehydration, the presence or absence of a mucilage layer is probably not involved in surviving short-term desiccation stress in *Klebsormidium*. However, the contribution of callose to survive water scarcity by restricting desiccation-induced

mechanical damage is indicated by three major findings: (i) the callose content in the cell walls increased strongly during desiccation stress; (ii) cellular water loss caused cell wall undulations allowing regulated shrinkage and expansion, with callose particularly abundant in the strained areas; and (iii) the cell wall of *Klebsormidium* lacks other cell wall components which allow cell wall flexibility (Sørensen et al. 2011).

Callose acts as a flexible supporter between individual cells of a Zygnema filament

We found that the cell walls of *Zygnema* contained less callose compared with *Klebsormidium*, and desiccation did not change their content. In contrast to *Klebsormidium*, desiccation forced the protoplasts of *Zygnema* to retract completely from the strongly expanded longitudinal cell walls, which prevents incorporation of callose into the walls as callose synthase is located in the plasma membrane. As *Zygnema* is closely related to land plants, the cell walls contain other flexibilizing components, such as AGPs, pectins and extensin (Sørensen et al. 2011). Cross cell walls, where the protoplast remains attached centrally after desiccation, only contain callose in cells with shorter longitudinal walls (i.e. recently divided cells), possibly indicating remnants of a newly formed septum after cytokinesis (Scherp et al. 2001). This callose accumulation has been found in numerous filament-forming or multicellular plants (Scherp et al. 2001); however, this has not been further investigated in the present study.

Most interestingly in *Zygnema*, AB labeling of semi-thin sections revealed callose to be restricted to cell corners between individual cells. In this area, biomechanical forces are greatest during desiccation, when the longitudinal walls expand convexly but the cross cell walls do not change their shape. The flexible callose-rich areas between the cells probablly act as supporters and help in dissipating shearing forces to avoid rupture of the load-bearing cell wall scaffold. The conspicuous deformation of the cellulose-rich longitudinal cell walls was already clearly visible after 30 min of desiccation, but, surprisingly, not lethal, as shown by microscopic Imaging-PAM by monitoring increasing photosynthetic performance after rehydration. Lacking full recovery of photosynthesis is in good agreement with previous findings showing young vegetative filaments of Zygnematophyceae to be more sensitive to water loss compared with Klebsormidiophyceae, which explains their preference for moister habitats (Holzinger and Karsten 2013). However, as a response to long-term desiccation or nutrient starvation, vegetative cells of *Zygnema* can be transformed into specialized resistant cells ('pre-akinetes' or akinetes), to increase the resistance against desiccation stress (Pichrtová et al. 2014a, Pichrtová et al. 2014b, Herburger et al. 2015). However, it is not clear whether *Klebsormidium* also forms such resistant cells (Mikhailyuk et al. 2014), and therefore the focus of this study was on comparing young vegetative filaments of *Zygnema* and *Klebsormi*dium that were fully metabolically active. Mucilage layers may be more or less abundant in different *Zygnema* species; however, culture age is a critical factor, where older cultures produce more mucilage (Herburger et al. 2015). Moreover, filaments obtained from polar field populations of *Zygnema* often produce fibrillose mucilage layers, which, in combination with the formation of extensive mats on the soil, protect against cellular water loss (Pichrtová et al. 2014b). The diameter of these pectic-rich layers increases when *Zygnema* is exposed to mild long-term desiccation stress (several months), which probably increases the water-holding capacity of the filaments during prolonged dry periods (Pichrtová et al. 2014b, and references therein). In contrast, the present study investigates the effects of severe short-term desiccation (30–210 min) on individual young filaments, resulting in retraction of the protoplast from the cell wall.

Callose allows terminal walls to expand convexly

In both *Zygnema* and *Klebsormidium*, high amounts of callose occur in terminal cell walls after fragmentation, which were expanded convexly due to the turgor pressure (Holzinger et al. 2011). Sufficient turgor pressure is also necessary for callose-rich rhizoid formation in detaching terminal cells of *Spirogyra* filaments (Yamada et al. 2003). Cell detachment was observed in *Zygnema* and *Klebsormidium*, while *K. nitens* showed the strongest tendency to fragment, which explains the highest callose content which probably positively correlates with the more frequent occurrence of terminal cross walls. In *Klebsormidium*, fragmentation into short filaments is commonly seen in liquid cultures (Rindi et al. 2008) and may have an ecological function (Karsten and Holzinger 2014). Fragmentation usually takes place along cross cell walls (Mikhailyuk et al. 2014), and remnants of wall material stay attached to newly exposed callose-rich cross walls. Imaging-PAM revealed that the photosynthetic performance of terminal cells in recently fragmented filaments of *Zygnema* and *Klebsormidium* and small filaments (2–3 cells) of *Klebsormidium* was not affected by cell detachment. Interestingly, in *Klebsormidium*, cell detachment is positively correlated with increasing light intensities or temperature under culture conditions (Dřímalová and Poulíčková 2003). Severe weather conditions entrain fragmented algal colonies into the atmosphere (Sharma et al. 2007). Therefore, we consider fragmentation into small and metabolically active [indicated by high Y(II)] filaments to be a fast and economic way for gaining dispersal units under changing environments (i.e. climate change). In part, this explains the worldwide distribution of *Klebsormidium* (Ryšánek et al. 2015).

Conclusion

Under natural conditions, a complex inter-relationship of many responses on the molecular and cellular level affects the ability of green algae to cope with water scarcity. In the present study, we focused on the cell wall and showed for the first time that desiccation stress nearly doubled the amount of callose even after 30 min desiccation in *Klebsormidium*, and callose localization is clearly evident in strained areas (cross walls). This correlates with a higher photosynthetic performance during desiccation and a full recovery after rehydration, while in *Zygnema* desiccation did not change the generally lower callose content and inhibited photosynthesis more strongly. Furthermore, the incorporation of callose in newly formed terminal cell walls may be a

prerequisite to survive the sudden rupture. Short algal filaments were found to be metabolically active [high Y(II)], considered to be important for dispersal and the global success of aero-terrestrial green algae. In future studies, a detailed investigation of AGPs and pectins of the Zygnematophyceae will increase our understanding of the current belief that this class is sister group to land plants (Wickett et al. 2014).

Materials and Methods

Algal material and culture conditions

Zygnema S (SAG 2419) and *Zygnema* E-A (SAG 2418) were isolated from aero-terrestrial habitats in different altitudes, and cultures were maintained in BBM (Bischoff and Bold 1963) in 250 ml Erlenmeyer flasks according to Herburger et al. (2015).

Klebsormidium crenulatum (SAG 2415) was isolated previously from the Schönwieskopf (Tyrol, Austria; Karsten et al. 2010), and *K. nitens* (SAG 2417; recently determined as *K. dissectum* according to Mikhailyuk et al. 2015) from concrete panels in the Botanical Garden of Innsbruck (Kaplan et al. 2012). Purified unialgal cultures were cultivated in modified BBM (3 NMBBM; Starr and Zeikus 1993) under the same conditions as described in the previous paragraph. Cell filaments of 4-week-old cultures were used in this study.

Desiccation experiments and colorimetric quantification of callose

Desiccation experiments were performed according to Karsten et al. (2014) in desiccation chambers at ambient humidity (AH; ~65%, monitored by a PCEMSR145 S-TH data logger; PCE Instruments) and room temperature (~21°C) at 40 µmol photons $m^{-2} s^{-1}$. Reproduciblility was guaranteed by using defined starting volumes of culture medium after removing excess moisture. For colorimetric quantification, fresh algae incubated in 200 µl of culture medium were spread evenly onto aluminum foil and desiccated for 0 (control), 30 or 210 min ($n = 4$). Particular care was taken in order to avoid mechanical stress or damage to the cells. Control and desiccated algae were then dried at 80°C for 13 h to remove the remaining water, and dry mass was then determined. Quantification of callose by using Aniline blue (Sigma-Aldrich) and a spectrofluorometer (QuantaMaster 300, HORIBA UK Ltd.) (excitation, 400 nm; emission, 510 nm) was performed according to Köhle et al. (1985). A calibration curve was established by using pachyman (Megazyme International), and the callose content in algae was expressed per µg of pachyman equivalents per mg of algal dry mass.

Light fluorescence and confocal laser scanning microscopy

Epifluosescence microscopy was performed with a Zeiss Axiovert 200M microscope (Carl Zeiss AG), equipped with a × 631.4 NA objective lens and a Zeiss Filter Set 01 (excitation, 365 nm; emission, 397 nm). Images were captured with an Axiocam MRc5 camera and Zeiss Axiovision software. For CLSM, a Zeiss Pascal CLSM system was used. All images were further processed with Adobe Photoshop (CS5) software version 12.1 (Adobe Systems).

Aniline blue and Calcofluor white staining

Single algal filaments and 1 µl of culture medium were transferred to welled slides, desiccated for 30 min and investigated by CLSM. Emission (long pass 560 nm) from a 488 nm excitation laser (argon) and a bright field image were collected in two channels. Callose and cellulose were stained with 1% Aniline blue and 1% Calcofluor white (Sigma-Aldrich), respectively (Krishnamurthy 1999). Both cellulose and callose were visualized by epifluorescence microscopy.

Immunocytochemistry

Live cell labeling was performed according to Domozych et al. (2011) and Eder and Lütz-Meindl (2010) with modifications. Cell filaments were washed and chemically fixed in PIPES buffer (pH 7.4) with 4% (v/v) paraformaldehyde (Sigma-Aldrich) and 1 mM $MgCl_2$ for 1 h. Filaments were washed in 1 ml of phosphate-buffered saline (PBS; 3 × 10 min), blocked in 2% bovine serum albumin (BSA; Sigma-Aldrich) and 0.1% Tween-20 (Sigma-Aldrich) in PBS for 30 min, washed again in 1 ml of PBS (3 × 10 min) and incubated for 2 h at room temperature in the primary AB (AB; 400-2; Biosupplies Australia Pty Ltd.; Meikle et al. 1991), 1 : 10 in PBS containing 0.1% Tween-20). Filaments were washed (1 ml of PBS, 3 × 10 min), incubated in the secondary AB [Alexa Fluor® 488 Goat Anti-Mouse IgG (γ1) (Life Technologies), 1 : 50 in PBS with 0.1% Tween-20] for 1.5 h at room temperature. Probes were transferred in Citifluor AF1 (Citifluor Ltd.) and examined by CLSM. Samples were excited at 488 nm (argon laser) and emission was collected in two separate channels at 505–550 nm (false color green) and long pass 560 nm (false color red). Z-stack projections were generated by overlaying several optical slices through half of the width or the whole cell filament.

Semi-thin sections (0.6–1.5 µm) of high pressure-frozen and freeze-substituted algal material (control and 210 min desiccated, see below) were prepared with a Leica Ultramicrotome (Leica Microsystems GmbH) and transferred to a 10-well polylysine-coated slide (ER-208B-AD-CE24, Thermo Scientific) previously cleaned with acetone. Sections were dried in the wells at 40°C for 60 min and blocked in 20 µl droplets of PBS containing 2.5% BSA and 0.05% Tween-20 for 45 min. Probes were rinsed (PBS) and covered with 20 µl droplets of the primary AB (400-2, 1 : 20 in PSB + 0.1% Tween-20) for 4.5 h at room temperature. After rinsing (PBS), probes were incubated in 20 µl droplets of the secondary AB (Alexa Fluor® 488 Goat Anti-Mouse IgG (γ1), 1 : 80 in PBS) for 3 h at room temperature. Probes were rinsed again (PBS), covered with Citifluor AF1 and excited at 488 nm. A corresponding bright field image was collected in a second channel. As a control, the primary AB was omitted.

Cryofixation and immunogold labeling

For cryofixation, algae and 200 µl of culture medium were transferred to a Ø 47 mm Whatman GF/F glass microfibre filter and desiccated for 210 min. Fresh and desiccated filaments were cryofixed in a Leica EMPACT high-pressure freezer (Leica Microsysteme) followed by freeze substitution (Leica EM AFS; Lütz-Meindl and Aichinger 2004) and embedding in LR-White (London Resin Company Ltd.). As cell walls in *Klebsormidium* are often multilayered (Mikhailyuk et al. 2014), additionally we used immunogold labeling to estimate whether callose occurs throughout the wall of hydrated filaments. Therefore, ultrathin sections were prepared by using a Leica ultramicrotome. Immunogold labeling and control experiments were performed according to Holzinger et al. (2000) with modifications. Briefly, ultrathin sections were blocked onto droplets of Tris buffer (50 mM, pH 7.5) containing 0.05% Tween-20 (TBST) and 2% BSA for 40 min at room temperature. Samples were transferred onto 20 µl droplets of the primary AB (400-2; 1 : 50 in TBST) for 16 h at 4°C. Samples were washed (droplets of TBST, 3 × 5 min) and stained with a 10 nm gold conjugated anti-mouse IgG AB (Sigma-Aldrich; 1 : 60 in TBST) for 2 h atroom temperature. Samples were rinsed (Tris buffer), placed onto droplets of TBST and rinsed again (Tris buffer and distilled water.). Samples were investigated using a Zeiss Libra 120 transmission electron microscope (80 kV) connected to a ProScan 2 k SSCCD camera, controlled with OSIS iTEM software.

Imaging-PAM

The microscopic version of an Imaging-PAM (M-series, Walz) was used to visualize the effective quantum yield of PSII [Y(II); false-colored image] and near infra red (NIR) remission (780 nm) in control, desiccated (30 min) and rehydrated (10, 60 and 180 min) algal filaments. Therefore, one filament of each strain was transferred to a welled slide and, after image generation (control) and coating with 1 µl of culture medium, desiccated for 30 min and imaged again. Subsequently, the same filament was rehydrated and investigated again after 10, 60 and 180 min of rehydration. This was repeated at least five times for each strain. Pictures were taken with a modified Axio ScopeA.1 epifluorescence microscope equipped with a Zeiss Fluar 40 × 1.3 (∞/0.17) objective lens and a IMAG-K6 CCD camera controlled with ImagingWinGigE (V2.45i) software. Measuring light for Y(II) determination was provided by an LED (620 nm). No special SP-Routine was applied to modify the signal/noise ratio.

Statistical evaluation of the data

Comparison of callose contents ($n = 4$) of control and desiccated (30 or 210 min) samples by using Origin 8.5 software (OriginLab Corporation) was evaluated by one-way analysis of variance (ANOVA) followed by Tukey's post-hoc test ($P < 0.001$) to find homogeneous subgroups of significantly different means.

Supplementary data

Supplementary data are available at PCP online.

Funding

The study was supported by a PhD scholarship from the University of Innsbruck, Austria ['Doktoratsstipendium neu, 3. Tranche 2013 to K.H.]; and The Austrian Science Fund (FWF) [projects P 24242-B16 and I 1951-B16 to A.H.].

Acknowledgements

We sincerely thank Professor M. Schagerl, University of Vienna, Biocenter, Austria, for allowing us to use his Imaging-PAM. Professor U. Lütz-Meindl, University of Salzburg, Austria, is acknowledged for providing access to her high-pressure freezing device. We also thank A. Andosch for the technical help in the high-pressure freezing and freeze substitution process, B. Jungwirth, University of Innsbruck, for help in transmission electron microcopy sectioning, and B. Waldboth, University of Innsbruck, for preliminary Aniline blue staining in various strains of *Klebsormidium*.

Disclosures

The authors have no conflicts of interest to declare.

References

Aigner, S., Remias, D., Karsten, U. and Holzinger, A. (2013) Unusual phenolic compounds contribute to ecophysiological performance in the purple colored green alga *Zygogonium ericetorum* (Zygnematophyceae, Streptophyta) from a high-alpine habitat. *J. Phycol.* 49: 648–660.

Andosch, A., Höftberger, M., Lütz, C. and Lütz-Meindl, U. (2015) Subcellular sequestration and impact of heavy mentals on the ultrastructure and physiology of the multicellular freshwater alga *Desmidium swartzii*. *Int. J. Mol. Sci.* 16: 10389–10410.

Bacic, A., Fincher, G.B. and Stone, B.A. (eds) (2009) Chemistry, Biochemistry, and Biology of 1–3 beta Glucans and Related Polysaccharides. Academic Press, Waltham, MA.

Bhuja, P., McLachlan, K., Stephens, J. and Taylor, G. (2004) Accumulation of 1, 3-β-D-glucans, in response to aluminum and cytosolic calcium in *Triticum aestivum*. *Plant Cell Physiol.* 45: 543–549.

Bischoff, H.W. and Bold, H.C. (1963) Phycological studies IV. Some soil algae from Enchanted Rock and related algal species. *Univ. Tex. Publ.* 6318: 1–95.

Brosch-Salomon, S., Höftberger, M., Holzinger, A. and Lütz-Meindl, U. (1998) Ultrastructural localization of polysaccharides and *N*-acetyl-D-galactosamine in the secretory pathway of green algae (Desmidiaceae). *J. Exp. Bot.* 49: 145–153.

Brown, D.H., Rapsch, S., Beckett, A. and Ascaso, C. (1987) The effect of desiccation on cell shape in the lichen *Parmelia sulcata* Taylor. *New Phytol.* 105: 295–299.

Cantarel, B.L., Coutinho, P.M., Rancurel, C., Bernard, T., Lombard. V. and Henrissat, B. (2009) The Carbohydrate-Active EnZymes database (CAZy): an expert resource for glycogenomics. *Nucleic Acids Res.* 37: 233–238.

Chen, X.Y. and Kim, J.Y. (2009) Callose synthesis in higher plants. *Plant Signal. Behav.* 4: 489–492.

Cook, M.E. (2004) Structure and asexual reproduction of the enigmatic charophycean green alga *Entransia fimbriata* (Klebsormidiales, Charophyceae). *J. Phycol.* 40: 424–431.

Domozych, D.S., Brechka, H., Britton, A. and Toso, M. (2011) Cell wall growth and modulation dynamics in a model unicellular green alga—*Penium margaritaceum*: live cell labeling with monoclonal antibodies. *J. Bot.* 2011: 1–8.

Domozych, D.S., Ciancia, M., Fangel, J.U., Mikkelsen, M.D., Ulvskov, P. and Willats, W.G.T. (2012) The cell walls of green algae: a journey through evolution and diversity. *Front. Plant Sci.* 3: 82.

Domozych, D.S., Kenneth, D.S. and Mattox, K.R. (1980) The comparative aspects of cell wall chemistry in the green algae (Chlorophyta). *J. Mol. Evol.* 15: 1–12.

Domozych, D.S., Lambiasse, L., Kiemle, S.N. and Gretz, M.R. (2009) Cell-wall development and bipolar growth in the desmid *Penium margaritaceum* (Zygnematophyceae, Streptophyta). Asymmetry in a symmetric world. *J. Phycol.* 45: 879–893.

Domozych, D.S., Serfis, A., Kiemle, S.N. and Gretz, M.R. (2007) The structure and biochemistry of charophycean cell walls: I. Pectins of *Penium margaritaceum*. Protoplasma *230: 99–115.*

Domozych, D.S., Sørensen, I., Popper, Z.A., Ochs, J., Andreas, A., Fangel, J.U. et al. (2014) Pectin metabolism and assembly in the cell wall of the charophyte green alga *Penium margaritaceum*. *Plant Physiol.* 165: 105–118.

Dong, X., Hong, Z., Sivaramakrishnan, M., Mahfouz, M. and Verma, D.P.S. (2005) Callose synthase (CalS5) is required for exine formation during microgametogenesis and for pollen viability in *Arabidopsis*. *Plant J.* 42: 315–328.

Dřímalová, D. and Poulíčková, A. (2003) Filament fragmentation of *Klebsormidium flaccidum*. *Biologia* 58: 525–527.

Eder, M. and Lütz-Meindl, U. (2008) Pectin-like carbohydrates in the green alga *Micrasterias* characterized by cytochemical analysis and energy filtering TEM. *J. Microsc.* 231: 201–214.

Eder, M. and Lütz-Meindl, U. (2010) Analyses and localization of pectin-like carbohydrates in cell wall and mucilage of the green alga *Netrium digitus*. *Protoplasma* 243: 25–38.

Eder, M., Tenhaken, R., Driouich, A. and Lütz-Meindl, U. (2008) Occurrence and characterization of arabinogalactan-like proteins and hemicelluloses in *Micrasterias* (Streptophyta). *J. Phycol.* 44: 1221–1234.

Eggert, D., Naumann, M., Reimer, R. and Voigt, C.A. (2014) Nanoscale glucan polymer network causes pathogen resistance. *Sci. Rep.* 4: 4159.

Elster, J. and Benson, E.E. (2004) Life in the polar terrestrial environment: a focus on algae and cyanobacteria. *In* Life in the Frozen State. Edited by Fuller, B., Lande, N. and Benson, E.E. pp. 111–150. CRC, London.

Graham, J.E., Wilcox, L.W. and Graham, L.E. (2009) Algae, 2nd edn. Benjamin Cummings, San Francisco.

Graham, L.E. and Taylor, C., III. (1986) Occurrence and phylogenetic significance of 'special walls' at meiosporogenesis in *Coleochaete*. *Amer. J. Bot.* 73: 597–601.

Gray, D.W., Lewis, L.A. and Cardon, Z.G. (2007) Photosynthetic recovery following desiccation of desert green algae (Chlorophyta) and their aquatic relatives. *Plant Cell Environ.* 30: 1240–1255.

Hall, J.D., McCourt, R.M. and Delwiche, C.F. (2008) Patterns of cell division in the filamentous desmidiaceae, close green algal relatives of land plants. *Amer. J. Bot.* 95: 643–654.

Hawes, I. (1990) Effects of freezing and thawing on a species of *Zygnema* (Chlorophyta) from the Antarctic. *Phycologia* 29: 326–331.

Herburger, K., Lewis, L.A. and Holzinger, A. (2015) Photosynthetic efficiency, desiccation tolerance and ultrastructure in two phylogenetically distinct strains of alpine *Zygnema* sp. (Zygnematophyceae, Streptophyta): role of pre-akinete formation. *Protoplasma* 252: 571–589.

Holzinger, A., Callaham, D.A., Hepler, P.K. and Meindl, U. (1995) Free calcium in *Micrasterias*: local gradients are not detected in growing lobes. *Eur. J. Cell Biol.* 67: 362–371.

Holzinger, A., Herburger, K., Kaplan, F. and Lewis, L.A. (2015) Desiccation tolerance in the chlorophyte green alga *Ulva compressa*: does cell wall architecture contribute to ecological success? *Planta* 242: 477–492.

Holzinger, A., Kaplan, F., Blaas, K., Zechmann, B., Komsic-Buchmann, K. and Becker, B. (2014) Transcriptomics of desiccation tolerance in the streptophyte green alga *Klebsormidium* reveal a land plant-like defense reaction. *PLoS ONE* 9: e110630.

Holzinger, A. and Karsten, U. (2013) Desiccation stress and tolerance in green algae: consequences for ultrastructure, physiological, and molecular mechanisms. *Front. Plant Sci.* 4: 327.

Holzinger, A., Lütz, C. and Karsten, U. (2011) Desiccation stress causes structural and ultra-structural alterations in the aeroterrestrial green alga *Klebsormidium crenulatum* (Klebsormidiophyceae, Streptophyta) isolated from an alpine soil crust. *J. Phycol.* 47: 591–602.

Holzinger, A., Mittermann, I., Laffer, S., Valenta, R. and Meindl, U. (1997) Microinjection of profilins from different sources into the green alga *Micrasterias* causes transient inhibition of cell growth. *Protoplasma* 199: 124–134.

Holzinger, A., Valenta, R. and Lütz-Meindl, U. (2000) Profilin is localized in the nucleus-associated microtubule and actin system and is evenly distributed in the cytoplasm of the green alga *Micrasterias denticulata*. *Protoplasma* 212: 197–205.

Hori, K., Maruyama, F., Fujisawa, T., Togashi, T., Yamamoto, N., Seo, M., et al. (2014) *Klebsormidium flaccidum* genome reveals primary factors for plant terrestrial adaptation. *Nat. Commun.* 5: 3978

Leliaert, F., Smith, D.R., Moreau, H., Herron, M.D., Verbruggen, H., Delchiche, C.F., et al. (2012) Phylogeny and molecular evolution of green algae. *Crit. Rev. Plant Sci.* 31: 1–46.

Iglesias, V.A. and Meins, F., Jr. (2000) Movement of plant viruses is delayed in a β-1,3-glucanase deficient mutant showing a reduced plasmodesmatal size exclusion limit and enhanced callose deposition. *Plant J.* 21: 157–166.

Kaplan, F., Lewis, L.A., Wastian, J. and Holzinger, A. (2012) Plasmolysis effects and osmotic potential of two phylogenetically distinct alpine strains of *Klebsormidium* (Streptophyta). *Protoplasma* 249: 789–804.

Kaplan, F., Lewis, L.A., Herburger, K. and Holzinger, A. (2013) Osmotic stress in the Arctic and Antarctic green alga *Zygnema* sp. (Zygnemtales, Streptophyta): effects on photosynthesis and ultrastructure. *Micron* 44: 317–330.

Karsten, U., Herburger, K. and Holzinger, A. (2014) Dehydration, temperature and light tolerance in members of the aeroterrestrial green algal genus *Interfilum* (Streptophyta) from biogeographically different temperate soils. *J. Phycol.* 5: 804–816.

Karsten, U. and Holzinger, A. (2014) Green algae in alpine biological soil crust communities: acclimation strategies against ultraviolet radiation and dehydration. *Biodivers. Conserv.* 23: 1845–1858.

Karsten, U., Lütz, C. and Holzinger, A. (2010) Ecophysiological performance of the aeroterrestrial green alga *Klebsormidium crenulatum* (Klebsormidiophyceae, Streptophyta) isolated from an alpine soil crust with an emphasis on desiccation stress. *J. Phycol.* 46: 1187–1197.

Karsten, U., Pröschold, T., Mikhailyuk, T. and Holzinger, A. (2013) Photosynthetic performance of different genotypes of the green alga *Klebsormidium* sp. (Streptophyta) isolated from biological soils crusts of the Alps. *Algol. Stud.* 142: 45–62.

Karsten, U. and Rindi, F. (2010) Ecophysiological performance of an urban strain of the aeroterrestrial green alga *Klebsormidium* sp. (Klebsormidiales, Klebsormidiophyceae). *Eur. J. Phycol.* 45: 426–435.

Krishnamurthy K.V. (1999) Methods in Cell Wall Cytochemistry. CRC Press, Boca Raton, FL.

Köhle, H., Jeblick, W., Poten, F., Blaschek, W. and Kauss, H. (1985) Chitosan-elicited callose synthesis in soybean cells as a Ca^{2+}-dependent process. *Plant Physiol.* 77: 544–551.

Lewis, L.A. and McCourt, R.M. (2004) Green algae and the origin of land plants. *Amer. J. Bot.* 91: 1535–1556.

Lütz-Meindl, U. and Aichinger, N. (2004) Use of energy-filtering transmission electron microscopy for routine ultrastructural analysis of high-pressure-frozen or chemically fixed plant cells. *Protoplasma* 223: 155–162.

Meikle, P.J., Bonig, I., Hoogenraad, N.J., Clarke, A.E. and Stone, B.A. (1991) The location of (1→3)-β-glucans in the walls of pollen tubes of *Nicotiana alata* using a (1→3)-β-glucan-specific monoclonal antibody. *Planta* 185: 1–8.

Menzel, D. (1988) How do giant plant cells cope with injury? The wound response in siphonous green algae. *Protoplasma* 144: 73–91.

Michel, G., Tonon, T., Scornet, D., Cock, J.M. and Kloareg, B. (2010) Central and storage carbon metabolism of the brown alga *Ectocarpus siliculosus*: insights into the origin and evolution of the storage carbohydrates in Eukaryotes. *New Phytol.* 188: 67–81.

Mikhailyuk, T., Glaser K., Holzinger, A. and Karsten, U. (2015) Biodiversity of *Klebsormidium* (Streptophyta) from alpine biological soil crusts (Alps, Tyrol, Austria and Italy). *J. Phycol.* 51: 750–767.

Mikhailyuk, T., Holzinger, A., Massalski, A. and Karsten, U. (2014) Morphology and ultrastructure of *Interfilum* and *Klebsormidium* (Klebsormidiales, Streptophyta) with special reference to cell division and thallus formation. *Eur. J. Phycol.* 49: 395–412.

Mikkelsen, M.D., Harholt, J., Ulvskov, P., Johansen, I.E., Fangel, J.U., Doblin, M.S., et al. (2014) Evidence for land plant cell wall biosynthetic mechanisms in charophyte green algae. *Ann. Bot.* 114: 1217–1236.

Moore, J.P., Farrant, J.M. and Driouich, A. (2008) A role for pectin-associated arabinans in maintaining the flexibility of the plant cell wall during water deficit stress. *Plant Signal. Behav.* 3: 102–104.

Moore, J.P., Nguema-Ona, E., Chevalier, L., Lindsey, G.G., Brandt, W.F., Lerouge, P., et al. (2006) Response of the leaf cell wall to desiccation in the resurrection plant *Myrothamnus flabellifolius*. *Plant Physiol.* 141: 651–662.

Moore, J.P., Nguema-Ona, E.E., Vicré-Gibouin, M., Sørensen, I., Willats, W.G.T., Driouich, A., et al. (2013) Arabinose-rich polymers as an evolutionary strategy to plasticize resurrection plant cell walls against desiccation. *Planta* 237: 739–754.

Nishikawa, S., Zinkl, G.M., Swanson, R.J., Maruyama, D. and Preuss, D. (2005) Callose (β-1,3 glucan) is essential for *Arabidopsis* pollen wall patterning, but not tube growth. *BMC Plant Biol.* 5: 22.

Peaucelle, A., Braybrook, S.A., Le Guillou, L., Bron, E., Kuhlemeier, C. and Höfte, H. (2011) Pectin-induced changes in cell wall mechanics underlie organ initiation in *Arabidopsis*. *Curr. Biol.* 21: 1720–1726.

Pichrtová, M., Hajek, T. and Elster, J. (2014a) Osmotic stress and recovery in field populations of *Zygnema* sp. (Zygnematophyceae, Streptophyta) on Svalbard (High Arctic) subjected to natural desiccation. *FEMS Microbiol. Ecol.* 89: 270–280.

Pichrtová, M., Kulichová, J. and Holzinger, A. (2014b) Nitrogen limitation and slow drying induce desiccation tolerance in conjugating green algae (Zygnematophyceae, Streptophyta) from polar habitats. *PLoS One* 9: e113137.

Popper, Z., Michel, G., Hervé, C., Domozych, D.S., Willats, W.G., Tuohy, M.G., et al. (2011) Evolution and diversity of plant cell walls: from algae to flowering plants. *Annu. Rev. Plant. Biol.* 62: 567–590.

Popper, Z. and Tuohy, M.G. (2010) Beyond the green: understanding the evolutionary puzzle of plant and algal cell walls. *Plant Physiol.* 153: 373–383.

Rindi, F., Guiry, M.D. and Lopez-Bautista, J.M. (2008) Distribution, morphology and phylogeny of *Klebsormidium* (Klebsormidiales, Charophyceae) in urban environments in Europe. *J. Phycol.* 44: 1529–1540.

Rindi, F., Mikhailyuk, T.I. Sluiman, H.J., Sluiman, H.J., Friedl, T. and López-Bautista, J.M., (2011) Phylogenetic relationships in *Interfilum* and *Klebsormidium* (Klebsormidiophyceae, Streptophyta). *Mol. Phylogenet. Evol.* 58: 218–231.

Ryšánek, D., Hrčková, K. and Škaloud, P. (2015) Global ubiquity and local endemism of free-living terrestrial protists: phylogeographic assessment of the streptophyte alga *Klebsormidium*. *Environ. Microbiol.* 17: 689–698.

Scheller, H.V. and Ulvskov, P. (2010) Hemicelluloses. *Annu. Rev. Plant Biol.* 61: 263–289.

Scherp, P., Grotha, R. and Kutschera, U. (2001) Occurrence and phylogenetic significance of cytokinesis-related callose in green algae, bryophytes, ferns and seed plants. *Plant Cell Rep.* 20: 143–149.

Sharma, N.K., Rai, A.K., Singh, S. and Brown, R.M. (2007) Airborne algae: their present status and relevance. *J. Phycol.* 43: 615–627.

Shephard, K.L. (1987) Evaporation of water from the mucilage of a gelatinous algal community. *Br. Phycol. J.* 22: 181–185.

Shi, X., Sun, X., Zhang, Z., Feng, D., Zhang, Q., Han, L., et al. (2014) GLUCAN SYNTHASE-LIKE 5 (GSL5) plays an essential role in male fertility by regulating callose metabolism during microsporogenesis in rice. *Plant Cell Physiol.* 56: 497–509.

Sørensen, I., Pettolino, F.A., Bacic, A., Ralph, J., Lu, F., O'Neill, M.A., et al. (2011) The charophycean green algae provide insights into the early origins of plant cell walls. *Plant J.* 68: 201–211.

Starr, R.C. and Zeikus. J.A. (1993) UTEX—the culture collection of algae at the University of Texas at Austin 1993 list of cultures. *J. Phycol.* 29: 1–106.

Timme, R.E., Bachvaroff, T.R. and Delwiche, C.F. (2012) Broad phylogenomic sampling and the sister lineage of land plants. *PLoS One* 7: e29696.

Vannerum, K., Huysman, M.J., De Rycke, R., Vuylsteke, M., Leliaert, F., Polliert, J., et al. (2011) Transcriptional analysis of cell growth and morphogenesis in the unicellular green alga *Micrasterias* (Streptophyta), with emphasis on the role of expansin. *BMC Plant Biol.* 11: 128.

Verma, D.P.S. (2001) Cytokinesis and building of the cell plate in plants. *Annu. Rev. Plant Physiol. Plant Mol. Biol.* 52: 751–784.

Vilumbrales, D.M., Skácelová, K. and Barták, M. (2013) Sensitivity of Antarctic freshwater algae to salt stress assessed by fast chlorophyll fluorescence transient. *Czech Polar Rep.* 3: 163–172.

Webb, M.A. and Arnott, H.J. (1982) Cell wall conformation in dry seeds in relation to the preservation of structural integrity during desiccation. *Amer. J. Bot.* 69: 1657–1668.

Wickett, N.J., Mirarab, S., Nguyen, N., Warnow, T., Carpenter, E., Matasci, N., et al. (2014) Phylotranscriptomic analysis of the origin and early diversification of land plants. *Proc. Natl. Acad. Sci. USA* 111: E4859–E4868.

Wodniok S., Brinkmann H., Glöckner G., Heidel A.J., Philippe H., Melkonian, M., et al. (2011) Origin of land plants: do conjugating green algae hold the key? *BMC Evol. Biol.* 11: 104.

Yamada, S., Sonobe, S. and Shimmen, T. (2003) Synthesis of a callosic substance during rhizoid differentiation in *Spirogyra*. *Plant Cell Physiol.* 44: 1225–1228.

Yin, Y., Johns, M.A., Cao, H. and Rupani, M. (2014) A survey of plant and algal genomes and transcriptomes reveals new insights into the evolution and function of the cellulose synthase superfamily. *BMC Plant Biol.* 15: 260.